This is a preprint, the final version is subject to change, of the American Mineralogist (MSA)
Cite as Authors (Year) Title. American Mineralogist, in press.
(DOI will not work until issue is live.) DOI: http://dx.doi.org/10.2138/am.2013.4273

Revision 1

Multinuclear NMR study of Cs-bearing Geyserites of the Targejia Hot Spring Cesium Deposit in Tibet

Bing Zhou[1, 2*], Erfeng Ren[2], Barbara L. Sherriff[3], Yefeng Yao[4]

1. College of Materials Science and Engineering, Tongji University, Shanghai, China, 201804
2. Qinghai Institute of Salt Lakes, Chinese Academy of Sciences, Xining, China, 810008
3. Department of Geological Sciences, University of Manitoba, Winnipeg, Manitoba, Canada R3T 2N2
4. Physics Department and Shanghai Key Laboratory of Magnetic Resonance, East China Normal University, Shanghai, China, 200062

*corresponding author: Bing Zhou umbingz1@hotmail.com

Key words: Cs-bearing geyserite deposits, Tibet, ^{29}Si, ^{133}Cs, ^{1}H MAS NMR, IR, silanol groups, mineralization.

Always consult and cite the final, published document. See http://www.minsocam.org or GeoscienceWorld

ABSTRACT

The large scale Targejia hot spring type Cs deposit in Tibet is unique and still active today with the distribution of hot springs being controlled by tectonic movements of the Tibetan Plateau. The ore bodies of the Targejia Cs deposit are mainly composed of geyserite, a Cs-containing opal. In this study, a combination of X-ray diffraction, infrared spectroscopy and ^{29}Si, ^{1}H, ^{133}Cs magic-angle spinning nuclear magnetic resonance (MAS NMR) were used to study the location and mobilization of Cs in geyserites. ^{29}Si NMR spectra indicate the relative amounts of Q^2, Q^3 and Q^4 species vary in geyserite samples of different mineralization stages. Based on the ^{133}Cs chemical shift as well as the change in ^{29}Si chemical shift ranges (especially for Q^2), cesium is inferred to associate with Q^3 and Q^2 silanol groups, where it is coordinated by O^{-2}, OH^- and H_2O as a network modifying cation. As Cs-bearing geyserite ages and dehydrates, Q^2 and Q^3 polymerize giving an increase in Q^4. This is accompanied with a decrease in Cs content indicating that Cs may be leached out from the opals as it loses its original coordination environment in the silicate framework.

Always consult and cite the final, published document. See http://www.minsocam.org or GeoscienceWorld

Introduction

The east-west-trending Himalayan Geothermal Zone in the Tibet Plateau is one of the most active geothermal areas on earth. It is distributed along the Yanglu Zangbo "suture line" between the Eurasian Plate to the north and the India Plate to the south, and is controlled by the subduction of the Indian Plate underneath the Tibetan Plateau. Geothermal activities in the Tibetan Plateau are typically in the form of hot springs, with varieties such as Si-, Ca-, S- and salt-rich geysers (Zheng 1995; Li et al. 2006). These hot springs are important not only for the study of the plateau evolution but also for the industrial utilization of geothermal energy and epithermal mineral deposits. Geothermal solutions from these hot springs are important sources for rare-metal mineralization in numerous saline lakes in Tibet (Zheng 1995). These hot springs and associated geothermal activities in the Tibet Plateau provide a unique natural laboratory for investigating modern epithermal mineralization and other ongoing ore-forming processes.

Cesium is an alkali metal that has been utilized widely in high-technology and military industries due to its excellent photon-electronic and chemical properties (Zheng 1995; Zhao et al. 2006, 2008). The unique hot spring Cs deposits in Tibet have a close genetic relationship with high-temperature geothermal anomalies, i.e., above 60 °C and with pH values of 8.5 to 9.0 (Shen et al. 2011). Due to the effects of the post Tibetan Plateau Collision, the geochemistry of these deposits is characterized by enrichments in B, Cs, Rb and Li (Zheng 1995; Zhao et al. 2006, 2008). Using electronic spin resonance (ESR) and other geochronological methods, the mineralization of Cs-bearing geyserite deposits at the Gulu and Targejia areas has been determined to have commenced around 0.5 Ma and remains

Always consult and cite the final, published document. See http://www.minsocam.org or GeoscienceWorld

active today (Zheng 1995; Zhao et al. 2006, 2008).

The mineral assemblages of the Cs-bearing geyserite deposits at the Gulu and Targejia areas are dominated by opals, which were precipitated from silica-rich solutions (Zheng 1995; Shen et al. 2011). Opals are hydrous minerals consisting of 150 to 300 nm diameter spheres of silica, which exhibit various degrees of structural disorder (Brown et al. 2003). Stages of opal solid-state transformations are commonly designated as opal-A (amorphous), opal-C (cristobalite) and opal-CT (cristobalite-tridymite), with the final stage being indicated by the presence of quartz (de Jong et al. 1987; Graetsch et al. 1994; Brown et al. 2003). Water is incorporated into the opal structure as molecular water (H_2O) and silanol (Si-OH) groups. Both vicinal ($SiO_3(OH)$, Q^3) and geminal ($SiO_2(OH)_2$, Q^2) hydroxyl groups are likely to occur at structural defects caused by incomplete polymerization of the silica tetrahedra, or at the surfaces of the silica spheres where the continuous silica network is interrupted (Paris et al. 2007). The solid-state transition between amorphous and crystalline opal should show up as variations in the local Si environments, which can be characterized by ^{29}Si nuclear magnetic resonance (NMR) spectroscopy, while the speciation and dynamic behavior of hydrogen in opals may be probed by ^{1}H NMR (Brown et al. 2003).

Here we combine X-ray diffraction (XRD), infra-red (IR) spectroscopy and magic-angle spinning (MAS) NMR spectroscopy to examine the structural sites occupied by Si, H and Cs in Cs-geyserites from the Targejia deposit. These data allow us to probe the local structure and connectivity among Si, H and Cs atoms. The atomic environment and migration behavior of Cs in Cs-geyserites will be discussed in this paper. The term “Cs-geyserite” will be used for the opal mineral assemblages of the Cs-bearing geyserite deposits at the Targejia area

Always consult and cite the final, published document. See http://www.minsocam.org or GeoscienceWorld

throughout this paper.

The Targejia Hot Spring Cesium Deposit

The largest hot spring type cesium deposit at the Targejia area is located in Ang Ren County of Tibet at an elevation of 5,000 m. Zheng (1995) reported a total reserve of ~1.446 x 10^4 T Cs with an ore grade up to 9.8 x 10^{-3} wt. %. Outcrops of Cs-geyserites at the Targejia deposit are in the forms of blocks (30 x 20 x 7 m^3), cones (radius 0.2-0.5 m; height 0.5-0.8 m), and veins (5-10 m long; 0.2-3 m wide). Individual ore-bodies are distributed at the surfaces along the fractures of Gangdise glacial moraine, or are situated on terraces and in river beds of the Changmaqu River. Mineralization at the Targejia Cs deposit has been classified into five stages from the top to the bottom of the terraces which have been dated by ESR and other methods (Zhao et al. 2006). The periods for the five stages of mineralization correspond to 255-201 ka, 99 ka, 39.4-25.0 ka, 14.8- 4.4 ka, and recent.

Cs-geyserites are composed of amorphous hydrous silica, which is mostly in a form of opal-CT for the early mineralization stages and opal-A for late stages. Granular opals exist through all stages, whereas coliform opals occur mainly in the late stages. Cauliflower-like, mega-grained massive and corrosion textures caused by dehydration processes are often observed in the early stages whereas fine-grained massive and porous textures are found only in the late stages. Other textural varieties such as clastic, stratiform, densely massive, stalactitic, colloidal, brecciated or conchoidal are also present (Zhao et al. 2006).

Geochemical analyses by Zheng (1995) showed that the Cs concentration at the Targejia deposit has an inverse correlation with the SiO_2 content and varies systematically with the age of mineralization. These relationships have been partly attributed to changes in the Cs and

Always consult and cite the final, published document. See http://www.minsocam.org or GeoscienceWorld

SiO_2 concentrations in the hot springs with time. Another contributing factor is the increase in the structural order of opals due to the progressive dehydration and polymerization of geyserites from the early to late mineralization stages (Zheng 1995; Zhao et al. 2006, 2008).

Materials and Methods

Sample preparation

Representative samples of Cs-geyserites from each of the five mineralization stages at the Targejia deposit were supplied by Dr. Yuanyi Zhao and Prof. Mianping Zhang. Samples 8-3-10-2, 8-3-10-3 are from initial stage of mineralization; 8-3-8-1, 8-3-5-1 and 8-3-5-2 belong to the second stage; third stage samples include 8-3-4-1, 8-3-4-2, 8-2-4-2 and 8-3-3-1; 8-3-1-1 and 8-3-1-3 are from the fourth stage; fifth stage mineralization samples are 8-3-2-7, 8-3-2-18, 8-3-2-26 and 8-3-2-30. Samples were various shades of gray, tan, light grayish-green or pink. The chemical compositions of the Cs-geyserite samples, which have been previously analyzed by energy spectra (Zhao et al. 2008), contain 90-98 wt. % SiO_2 and 0.6-2.6 wt. % Cs_2O (Table 1).

Opals from these samples were handpicked under a binocular microscope and then ground to fine powders using an agate mortar and pestle for XRD, IR and MAS NMR spectroscopy. Samples with high Cs content are chosen for ^{133}Cs MAS NMR experiments.

In order to investigate the structural changes as opal ages, a geyserite sample was subjected to high energy ultrasonic vibration in an attempt to speed up the polymerization processes. A portion of 3rd stage Cs-geyserite sample 8-3-4-2 (0.3 g) was immersed in 4 mL of $NaHCO_3$ solution (pH = 8.5), then stirred by high energy ultrasonic vibration (KQ-100DB NC Ultrasonic Cleaner) for six hours, and finally dried in an oven at 80 °C for a further six hours

Always consult and cite the final, published document. See http://www.minsocam.org or GeoscienceWorld

before NMR analysis.

X-ray diffraction

Powder XRD data were collected at room temperature with a computer-controlled Bruker D8 Advance Diffractometer (Chinese Academy of Geological Sciences) using Cu K_α radiation in a step width of 0.02° for Δ2θ and a 2θ range from 10 to 70°, with scanning speed of 3°/min and count time of 5 s per step.

IR spectroscopy

Hand-picked opals were ground to a fine powder and combined with KBr (99.9%) and pressed into pellets. IR absorption spectra were recorded at room temperature on a Perkin-Elmer 580 double-beam IR spectrometer with a wave number range from 400 cm^{-1} to 4000 cm^{-1}, and a 4 cm^{-1} resolution (Chinese Academy of Geological Sciences, and Shanghai Key Laboratory of Magnetic Resonance).

MAS NMR Spectroscopy

^{29}Si MAS NMR experiments were measured on Bruker DSX-300 spectrometer (B_o = 7.05 T) using a 7 mm Bruker MAS probe (Shanghai Key Laboratory of Magnetic Resonance). Samples were packed within ZrO_2 rotors (7.0 mm outer diameter (o.d.)) and spun to 3,000 Hz. Decoupled Bloch ^{29}Si MAS NMR spectra were acquired with a recycle delay time of 120 s and ^{1}H decoupling with a ν_{rf} of 50 kHz was applied during the acquisition. The ^{1}H-^{29}Si cross polarization (CP) MAS NMR spectra were acquired using a contact time of 2 ms. The Bloch decay and CP experiments were acquired using between 200 and 2,048 co-added transients.

^{29}Si MAS NMR experiments were also acquired using a Bruker Avance III 500 (B_o = 11.74 T) spectrometer with a triple-resonance Bruker broadband probe (Department of

Always consult and cite the final, published document. See http://www.minsocam.org or GeoscienceWorld

Chemistry, University of Manitoba). Samples were packed in 3.2 mm ZrO_2 rotors (22 μL sample volume) and a spinning frequency between 4,200 and 8,000 Hz used. ^{29}Si spectra were acquired using both Bloch decay (average recycle delay of 60 s) and CP experiments (with a recycle delay of 2 s, and contact time of 2 ms), and between 13,000 and 20,000 co-added transients. The geyserite sample recorded were a faint pink/purple in color suggesting trace amounts of paramagnetic impurities, likely Mn. The recycle delays for CP experiments were determined from ^{1}H spin-lattice experiments, while ^{29}Si Bloch experiments were recorded at 30, 60, 120 and 300 seconds using a tip angle of 30^{o}. ^{29}Si NMR spectra were referenced to 6.68 ppm using hexamethylsiloxane as a secondary external reference relative to TMS (0.0 ppm).

^{1}H Bloch decay and DQ-filtered MAS NMR spectra were also acquired on a Bruker DSX-600 spectrometer (B_o =14.1 T) using a 2.5 mm Bruker MAS probe (Shanghai Key Laboratory of Magnetic Resonance). The Bloch decay ^{1}H MAS NMR spectra were acquired with a recycle delay time of 4 s and a spinning frequency of 25,000 Hz. The DQ-SQ sequence was used for the ^{1}H DQ-filtered NMR experiments (Schnell and Spiess 2001) with 80 μs for both the excitation and reconversion time, and MAS spinning frequencies were 25,000 Hz with a ν_{rf} of 37 kHz. Chemical shifts for ^{1}H was referenced to tetramethylsiliane (TMS) to 0.00 ppm.

^{133}Cs MAS NMR spectra were acquired using a Varian ^{UNITY}Inova 600 (B_o =14.1 T) spectrometer with a 5 mm double resonance Varian-Chemagnetics probe (H/F-X) (Department of Chemistry, University of Manitoba). A hand-picked opal sample was ground to a fine powder and packed into a 5 mm outer diameter Si_3N_4 rotor (140 μL sample volume).

Always consult and cite the final, published document. See http://www.minsocam.org or GeoscienceWorld

Bloch decay (40^o tip-angle) and Hahn-echo ($\pi/2$-τ-π, π = 8 μs) spectra were acquired using 50,000 co-added transients, 5 s recycle delays and a spinning frequency of 10,500 Hz. Spectra were referenced to 0.5 M CsCl (0.00 ppm). In previous studies (Kroeker et al. 2010), crystalline synthetic cesium-containing oxides were determined to show long spin-lattice relaxation times (e.g., 100s of seconds), therefore, caution was taken when studying Cs-containing oxides. In this study, the absence of highly crystalline Cs sites was checked using recycle delays of 8 minutes over a period of 3 to 4 days. Again, a small fraction of paramagnetic transition metals assisted in shortening the relaxation times (spin-lattice), enabling short recycle delays.

Results and Discussion

Characterization of the samples by XRD and IR

All of the samples were analyzed by XRD and IR. Representative XRD results (Fig. 1) show that the samples from the first two stages (8-3-10-3, 8-3-8-1) are characterized by a higher degree of crystallization indicated by quartz peaks whereas the last stage sample is an amorphous SiO_2 phase (opal) (8-3-2-18). The XRD pattern of 8-3-4-1 indicates that the third stage is mainly composed of opal-A with minor quartz. Minor amounts of clastic plagioclase, orthoclase as well as quartz were found within the fourth stage Cs-geyserite sample (8-3-1-1). Overall the XRD patterns (Fig. 1) show a general trend from early to late stages, with decreases in the degree of crystallization and increases in opal-A.

In the IR spectra, the bending vibration absorbance bands at 798 cm^{-1}, 694 cm^{-1} and 472 cm^{-1}, which are typical of opals (Zheng 1995), are present in the samples 8-3-10-2 (1^{st} stage), 8-3-8-1 (2^{nd} stage) and 8-3-2-18 (5^{th} stage) (Figs. 2a and 2b). These bands can be assigned to

Always consult and cite the final, published document. See http://www.minsocam.org or GeoscienceWorld

tetrahedrally coordinated silicon (Graetsch et al. 1994) together with the intense band at approximately 1100 cm^{-1} present in the IR spectra for all the samples (Fig. 2a). The absorbance band near 620 cm^{-1}, which is characteristic of low-cristobalite (Etchepare et al. 1978; Graetsch et al. 1994), is absent in these IR spectra (Figs. 2a and 2b) indicating that the Cs-geyserite samples in this study are mainly opal-CT and opal-A. The IR spectra of opal-CT and opal-A differ only in the width and line-shape of the absorption bands (Fig. 2a) with an increase in the bandwidth at the region 3500 cm^{-1} and for the peaks at smaller wavenumbers occurring in the order opal-C, opal–CT and opal-A.

In summary, the XRD and IR data show that the minerals of the Targejia Cs deposit in Tibet are mainly composed of opal-A and opal-CT with small amounts of quartz present in samples 8-3-10-2 (1^{st} stage), 8-3-3-1 and 8-3-1-1 (both 4^{th} stage), with minor plagioclase and orthoclase also detected in the latter two samples.

MAS NMR Spectroscopy and structural implications

Bloch decay ^{29}Si MAS NMR spectra at both 7.05 T and 11.74 T show a main resonance centered at -111 ppm, with a full width at half maximum (FWHM) of ~9.5 ppm (Fig. 3a) and a shoulder on the left-hand side (i.e., to higher frequency). The resonance at -111 ppm is characteristic of Q^4 structural arrangements (all bridging oxygens) in amorphous silica (Engelhardt and Michel 1987; de Jong et al. 1987). This chemical shift is between the experimental chemical shifts for cristobalite and tridymite (de Jong et al. 1987). According to Chemtob et al. (2012), too short of a recycle delay time may result in significant underestimation of Q^4 but the delay times of 60 and 120s used for these experiments are believed to be sufficient to eliminate this problem. The asymmetrical shoulder observed on

Always consult and cite the final, published document. See http://www.minsocam.org or GeoscienceWorld

the left-hand side can be explained by the additional overlapping resonances from silanol groups, Q^3 ($SiO_3(OH)$) and Q^2 ($SiO_2(OH)_2$). The width of the ^{29}Si MAS NMR resonances in the Cs-geyserites is caused by a distribution of silica species that vary in both bond distances and Si-O-Si angles. Such distribution represents a significant extent of relative local disorder (de Jong et al. 1987; Brown et al. 2003). The empirical equation $\delta_{iso} = -19.8215 - 0.608526$ (<θ>) can be used to correlate ^{29}Si chemical shift (ppm) with average <Si-O-Si> angle (<θ>) (Thomas et al. 1983). This equation gives <θ> for Q^4 of 151.5°, which is between the values of 151° for opal-A and 152° for opal-CT previously determined by de Jong et al. (1987).

^1H-^{29}Si CP MAS NMR spectroscopy resolves the higher frequency shoulder into multiple resonances around -101 ppm and -90 ppm (Figs. 3b and 4). The intensity of the main resonance (-111 ppm) detected by the Bloch decay experiment decreases relative to the newly resolved resonances for the Cs-geyserites of all mineralization stages (Fig. 3b and 4). The relative intensity for Q^4 units suffers in CPMAS spectra because the longer distances to -OH result in poor ^1H spin-transfer to ^{29}Si, in contrast to the proximity of the hydroxyl (OH) groups in Q^3 and Q^2 silanol groups, which enable more efficient magnetization transfer. The resonance at -101 ppm is assigned to Q^3 vicinal silanol groups, and the resonance ~ -90 ppm to Q^2 geminal silanol groups. For Q^4 and Q^3 species, both isotropic chemical shifts and FWHM of 9.5 ppm agree well with published results for opals (Brown et al. 2003).

The presence of Q^2 and Q^3 silanol groups with protons attached to the non-bridging oxygen agrees with research showing that most of the water present within the Cs-geyserites is chemisorbed (Graetsch et al. 1994; Paris et al. 2007).

The line-shapes of ^1H-^{29}Si CPMAS spectra for the geyserite samples at each

Always consult and cite the final, published document. See http://www.minsocam.org or GeoscienceWorld

234 mineralization stage are similar; however, there are variations of the relative intensity ratios
235 for the Q^2, Q^3 and Q^4 environments for different samples, and for different slices through the
236 same sample, indicating the evolution of geyserites. For example, the relative intensity for the
237 Q^4 resonance located in the lower section of Sample 8-3-4-2 (3^{rd} stage) is lower than that for
238 the upper and middle sections of the same sample (Fig. 4).

239 ^{1}H DQ-filtered experiments are often used to detect ^{1}H resonances from strong correlated
240 ^{1}H-^{1}H dipolar interactions (i.e., hydrogen bonding), whereas the Bloch experiment excites all
241 the ^{1}H environments equally within a sample (Schnell 2004; Paris et al. 2007). The ^{1}H MAS
242 NMR spectrum of Sample 8-3-2-30 (5^{th} stage) exhibits three resonances: an intense narrow
243 resonance around 4 ppm with a FWHM of 2-3 ppm, a broad shoulder between 6.5 and 8 ppm
244 and a narrow, less intense resonance at 0.9 ppm (Figs. 5a and 5b). ^{1}H resonances located
245 below 1.8 ppm usually are assigned to internal isolated silanols with very weak or no
246 hydrogen-bonding (Hansen et al. 2008, 2009; Paris et al. 2007). Therefore, the resonance
247 located at 0.9 ppm is assigned to weakly hydrogen-bonded or to isolated hydroxyls associated
248 with Q^2/Q^3 environments. The dominant peak at ~4 ppm is assigned to water within geyserite
249 (Paris et al. 2007). ^{1}H NMR peaks above 7 ppm correspond to the protons strongly bonded to
250 the non-bridging oxygen atoms (Hansen et al. 2008, 2009; Xue and Kanzaki 2009), therefore,
251 the broad shoulder between 6.5 and 8 ppm may result from strong hydrogen-bonded
252 hydroxyls, internal Q^2 and Q^3 silanols, residual physisorbed water molecules, or Cs
253 environments such as Si-OH---Cs. These assignments are consistent with those in opals by
254 Paris et al. (2007). ^{1}H spins in geyserite are present either in the form of "free" water which is
255 not in a correlated dipolar state due to the mobility, or hydrogen-bonded where the ^{1}H spins

Always consult and cite the final, published document. See http://www.minsocam.org or GeoscienceWorld

256 are strongly correlated. The relative intensities of ^{1}H DQ-filtered spectrum are scaled by the
257 magnitude of the homonuclear dipole–dipole couplings that the respective ^{1}H spin
258 experiences (Schnell et al. 2001; Paris et al. 2007).

259 The assignments of ^{1}H NMR peaks were verified by the DQ-filtering effect, as this
260 causes intensity from the mobile water resonance to decrease, while signals from stronger
261 hydrogen-bonded hydroxyls and internal Q^2 and Q^3 silanols are enhanced (Fig. 5c). The cross
262 peak in DQ-filtered 2D ^{1}H NMR spectrum of the 5th stage Sample 8-3-2-30 (Fig. 5d) indicates
263 a correlation between water (4.6 ppm) and the stronger hydrogen-bonded hydroxyls (above
264 6.5 ppm). Therefore, some water within geyserites is near OH groups, interacting with these
265 groups through hydrogen bonding. The peak at 4.6 ppm of the DQ spectrum becomes broader
266 than the corresponding peak of MAS NMR due to the signals from both mobile as well as less
267 mobile water (Fig. 5).

268 Cesium-133 (I=7/2) is a useful nucleus for NMR study due to its 100% natural abundance,
269 and a moderate gyromagnetic ratio (γ) (Kim et al. 1996a, 1996b; Weiss et al. 1990a, 1990b;
270 Ejeckam and Sherriff 2005). Because of the small quadrupolar moment of ^{133}Cs and the high
271 magnetic field (14.1 T) used here, ^{133}Cs resonances do not show the characteristic
272 singularities of second-order broadening of the central transition. As the second-order
273 quadrupolar interaction induces a shift of less than 11 Hz for ^{133}Cs, the center-of-gravity of
274 the resonance can be taken as an isotropic chemical shift (Michaelis et al. 2007, 2009 ;
275 Kroeker et al. 2003, 2006). The large number of electrons causes Cs nucleus to be very
276 polarizable with a wide chemical shift range of 350 ppm (Mason 1987; Michaelis et al. 2007;
277 Michaelis and Kroeker 2009; Weiss et al. 1990a, 1990b) and hence sensitive to small changes

Always consult and cite the final, published document. See http://www.minsocam.org or GeoscienceWorld

in local structures.

The ^{133}Cs MAS NMR spectra of Cs geyserites have a single broad Gaussian shaped resonance centered at ~ -40 ppm with a FWHM of 9 ppm (Fig. 6). The lack of additional narrow resonances in ^{133}Cs MAS NMR spectrum due to crystalline Cs, together with optical microscopic observations, and IR and XRD analyses indicates that there are no independent Cs minerals in these samples (Kroeker et al 2010, Greer and Kroeker 2012). The ^{133}Cs chemical shift of ~-40 ppm precludes the hydration of Cs in Cs-geyserites because ^{133}Cs chemical shift for Cs species in solution ranges from 0 to 69 ppm (Mason 1987; Weiss et al. 1990a, 1990b).

The negligible content of trivalent cations such as Al in Cs-geyserite precludes Cs from being a charge balancing cation. Unlike strongly hydrated cations such as Li, Ca and Mg, weakly hydrated cations such as K and Cs are expected to come into direct contact with the defects (surfaces) within the opal structure (Kim et al. 1996a, 1996b; Weiss et al. 1990a, 1990b). Therefore, the ^{133}Cs chemical shift observed for Cs-geyserites is neither caused by separate Cs minerals nor by Cs surrounded by a complete hydration shell. It is likely to arise from Cs in structural environments similar to the Stern Layer in clay minerals, where Cs is located at Q^2 and Q^3 sites caused by structural defects or surfaces (Weiss et al. 1990a, 1990b; Kim et al. 1996a, 1996b; Ejeckam and Sherriff 2005).

Cesium in such environments is tightly bound to and coordinated by O atoms of the Si tetrahedra, and may also be surrounded by some water molecules which interact with stronger hydrogen-bonded hydroxyls or internal silanol groups as shown by ^{1}H NMR spectra. As a result, the chemical shifts around -90 ppm for Q^2 in Cs-geyserite samples would be shifted

Always consult and cite the final, published document. See http://www.minsocam.org or GeoscienceWorld

toward to higher field compared with those for the Q^2 environments without adjacent Cs.

Due to the size of the Cs cation, the coordination environment can vary significantly and may be probed via NMR. ^{133}Cs, $^{6/7}Li$, ^{23}Na, ^{27}Al and ^{29}Si resonances have been shown to shift to lower frequency (i.e., more shielded) with an increase in coordination number for ionic solids (Smith and Blackwell 1983; Xu and Stebbins 1995; Michaelis et al. 2007). Weiss et al. (1990a) assigned a ^{133}Cs peak at ~56 ppm to hydrated Cs sites with a coordination number of 9. The resonance centered at -40 ppm in Fig. 6 is probably from the 10- to 12-fold Cs polyhedron mainly coordinated by OH and basal O atoms of the SiO_4 tetrahedron.

Thermodynamic calculations show that the hydrated silica series composed of $Si(OH)_4$ tetrahedra have much weaker bonding between Si and OH than for Si-O (Zheng 1995). Based on the principles of hydrothermal mineralization and colloid chemistry, Zheng (1995) asserted that strong electrolyte alkaline elements such as Cs can accelerate the precipitation of colloidal hydrous SiO_2 and form opals. Such a precipitation process leads to the incomplete poly-condensation of silica tetrahedra and forms silica spheres. The surfaces of silica spheres can also interrupt the continuous silica network. This can result in the formation of both vicinal and geminal hydroxyl groups. The hydroxyl groups terminating Si tetrahedra in Cs-geyserite cause local negative charges at the internal structural defects or near the surface of silica spheres in Cs-geyserites, which are not fully balanced by Si^{4+}. Cs^+ is then attracted electrostatically by the negative charges resulting in Cs adsorption at defect or surface of Q^2, Q^3 sites (silanol groups), therefore, Cs is most likely located at Q^2, Q^3 sites in geyserites, and connected tightly with the Si network of opals.

As the opals age, the SiO_4 tetrahedra coalesce and polymerize, then opal-A evolves to

Always consult and cite the final, published document. See http://www.minsocam.org or GeoscienceWorld

322 opal-CT or quartz, so the structure becomes more ordered and will eventually crystallize.
323 Such structural reorganization results in the loss of 'bound' water and silanol groups (Paris et
324 al. 2007). Sample 8-3-4-2 (3rd stage) was used in an attempt to accelerate such a
325 polymerization process by subjecting the sample to high energy ultrasonic vibration before
326 running a second ^{1}H-^{29}Si CP MAS NMR spectrum. The intensity for the Q^4 peak in the 3rd
327 stage Sample 8-3-4-2 (Fig. 7) is shown to increase after this ultrasonic vibration process. This
328 change possibly results from the reaction of Si-OH + HO-Si ↔ Si-O-Si + H_2O. As a result of
329 such a solid-state transition in Cs-geyserite, Cs may lose its coordination environments and be
330 leached out during the progressive polymerization process as opals age.

331 In summary, ^{29}Si MAS and ^{1}H-^{29}Si CP MAS spectra reveal the main structural unit in
332 Cs-geyserites is Q^4 silicon tetrahedra, with limited amounts of Q^3 and Q^2 species.
333 Characterization of the hydroxyl groups was achieved using NMR chemical shift information,
334 ^{1}H-^{29}Si CPMAS and DQ-filtered ^{1}H spectra. ^{133}Cs MAS NMR spectroscopy suggests that Cs
335 in Cs-geyserites is associated with silanol groups and is coordinated mainly by OH and basal
336 O atoms of silicate tetrahedra, rather than being in separated phases such as crystalline Cs
337 oxides or fully hydrated Cs coordination. ^{1}H-^{29}Si CP MAS NMR spectra before and after
338 ultrasonification indicate the process of SiO_4 coalescence and polymerization in Cs-geyserites.
339 Leaching of Cs during such a process, may be the reason for Cs concentration decreasing with
340 aging.

341

342 **Acknowledgements:** The authors would like to thank Dr. Yuanyi Zhao and Prof. Mianping
343 Zhang from the Chinese Academy of Geological Sciences for providing Cs-geyserite samples

Always consult and cite the final, published document. See http://www.minsocam.org or GeoscienceWorld

from private collections. Dr. K. Marat is thanked for valuable discussion during the course of this research. The research grant "One Hundred People Plan" has been provided by Chinese Academy of Sciences (B.Z.). Y.Y. acknowledges financial support from NSFC grant no. 21174039. We are grateful to Drs. Vladimir Michaelis and Scott Kroeker (University of Manitoba) for collecting ^{133}Cs and ^{29}Si NMR spectra on selected samples and insightful discussions, and revisions to an earlier version of this paper. NSERC is acknowledged for a Major Resources Support grant to the University of Manitoba. The authors also acknowledge the helpful comments from anonymous reviewers of this manuscript.

Always consult and cite the final, published document. See http://www.minsocam.org or GeoscienceWorld

352 **References:**

353 Brown, L., Ray, A., and Thomas, P. (2003) ^{29}Si and ^{27}Al NMR study of amorphous and
354 paracrystalline opals from Australia. Journal of Non-Crystalline Solids, 332, 242-248.
355 Chemtob, S.M., Rossman, G.R., and Stebbins, J.F. (2012) Natural hydrous amorphous silica:
356 quantitation of network speciation and hydroxyl content by ^{29}Si MAS NMR and
357 vibrational spectroscopy. American Mineralogist, 97, 203 -211.
358 de Jong, B., Hoek, J., Veeman, W., and Mason, D. (1987) X-ray diffraction and ^{29}Si
359 magic-angle-spinning NMR of opals: Incoherent long- and short-range order in opal-CT.
360 American Mineralogist, 72, 1195-1203.
361 Etchepare, J., Merian, M., and Kaplan, P. (1978) Vibrational normal modes of SiO_2. II.
362 Cristobalite and tridymite. Journal of Physical Chemistry, 68, 1531-1537.
363 Ejeckam R.B., and Sherriff, B.L. (2005) A^{133}Cs, ^{29}Si and ^{27}Al MAS NMR spectroscopic study
364 of Cs absorption by clay minerals: implications for the disposal of nuclear waste.
365 Canadian Mineralogist, 43**,** 1131-1140.
366 Engelhardt, G., and Michel, D. (1987) High-resolution solid-state NMR of silicates and
367 zeolites. John Wiley & Sons, New York.
368 Graetsch, H., Gies, H., and Topalovic, I. (1994) NMR, XRD and IR study on microcrystalline
369 opals. Physics and Chemistry of Minerals, 21, 166-175.
370 Greer, B.J., and Kroeker, S. (2012), Characterisation of heterogeneous molybdate and
371 chromate phase assemblages in model nuclear waste glasses by multinuclear magnetic
372 resonance spectroscopy. Physical Chemistry Chemical Physics, 14, 7375-7383.
373 Hansen, M.R., Jakobsen, H.J., and Skibsted, J. (2008) Structural environments for boron and

Always consult and cite the final, published document. See http://www.minsocam.org or GeoscienceWorld

aluminum in alumina-boria catalysts and their precursors from ^{11}B and ^{27}Al single- and double-resonance MAS NMR experiments. Journal of Physical Chemistry, 112, 7210-7222.

Hansen, M. R., Jakobsen, H.J., and Skibsted, J. (2009) Structure and dynamics of hydrous surface species on alumina-boria catalysts and their precursors from ^{1}H, ^{2}H, ^{11}B and ^{27}Al MAS NMR spectroscopy. Journal of Physical Chemistry, 113, 2475-2486.

Kim, Y., Cygan, R., and Kirkpatrick, R.J. (1996a) ^{133}Cs NMR and XPS investigation of cesium absorbed on the clay minerals and related phases. Geochimica et Cosmochimica Acta, 60, 1041-1052.

Kim, Y., Kirkpatrick, R. J., and Cygan, R. (1996b) ^{133}Cs NMR study of cesium on the surfaces of kaolinite and illite. Geochimica et Cosmochimica Acta, 60, 4059-4074.

Kroeker, S., Feller, S.A., Affatigato, M., O'Brien, C.P., Clarida, W.J., and Kodama, M. (2003) Multiple four coordinated boron sites in caesium borate glasses and their relation to medium range order. Physics and Chemistry of Glasses, 44, 54-58.

Kroeker, S., Aguiar, P.M., Cerquiera, A., Okora, J., Clarida, W., Doerr, J., Olesiuk, M., Ongie, G., Affatigato, M., and Feller, S.A. (2006) Alkali dependence of tetrahedral boron in alkali borate glasses. Physics and Chemistry of Glasses- European Journal of Glass Science and Technology, B47, 393-396.

Kroeker, S., Higman, C.S., Michaelis, V.K., Svenda, N.B., and Schuller, S. (2010) Precipitation of Mixed-Alkali Molybdates During HLW Vitrification. Material Research Society Symposium Proceedings, 1265, 1265-AA03-03.

Li, Z., Hou, Z., Nie, F., and Yang, Z. (2006) Enrichment of element Cesium during modern

Always consult and cite the final, published document. See http://www.minsocam.org or GeoscienceWorld

geothermal action in Tibet, China. Acta Geologica Sinica, 80, 1457-1464.

Mason, E. (1987) Multinuclear NMR. Plenum Press, New York.

Michaelis, V.K., Aguiar, P.M., and Kroeker, S. (2007) Probing alkali coordination environments in alkali borate glasses by multinuclear magnetic resonance. Journal of Non-Crystalline Solids, 353, 2582-2590.

Michaelis, V.K., and Kroeker, S. (2009) Caesium volatilization in borosilicate glasses: a multinuclear magnetic resonance study. Physics and Chemistry of Glasses: European J. of Glass Science and Technology, B50, 249-252.

Paris, M., Fritsch, E., and Reyes, B.O. (2007) ^{1}H, ^{29}Si and ^{27}Al NMR study of the destabilization process of a paracrytalline opal from Mexico. Journal of Non-Crystalline Solids, 353, 1650-1656.

Schnell, I., and Spiess, H.W. (2001) High-Resolution ^{1}H NMR Spectroscopy in the Solid State: Very Fast Sample Rotation and Multiple-Quantum Coherences. Journal of Magnetic Resonance, 151, 153-227.

Schnell, I. (2004) Dipolar recoupling in fast-MAS solid-state NMR spectroscopy. Progress in Nuclear Magnetic Resonance Spectroscopy, 45, 145-207.

Shen, L., Wu, K., Xiao, Q., and Yuan, D. (2011) Carbon dioxide degassing flux from two geothermal fields in Tibet, China. Chinese Science Bulletin, 56, 1-11.

Smith, J.V., and Blackwell, C.S. (1983) Nuclear magnetic resonance of silica polymophs. Nature, 303, 223-225.

Thomas, J.M., Klinowski, J., Ramdas, S., Hunter, B.K., and Tennakoon, D.T.B. (1983) The evaluation of nonequivalent tetrahedral sites from silicon-29 NMR chemical shifts in

Always consult and cite the final, published document. See http://www.minsocam.org or GeoscienceWorld

418 zeolites and related aluminosilicates. Chemical Physics Letters, 102, 158-162.

419 Weiss, C., Kirkpatrick, R.J., and Altaner S.P. (1990a) Variations in interlayer cation sites of
420 clay minerals as studied by ^{133}Cs MAS nuclear magnetic resonance spectroscopy.
421 American Mineralogist, 75, 970-982.

422 Weiss, C., Kirkpatrick, R.J., and Altaner S.P. (1990b) The structural environments of cations
423 adsorbed onto clay: ^{133}Cs variable-temperature MAS NMR spectroscopy study of
424 hectorite. Geochimica et Cosmochimica Acta, 54, 1655-1669.

425 Xu, Z., and Stebbins, J.F. (1995) ^{6}Li Nuclear magnetic resonance chemical shifts,
426 coordination number and relaxation in crystalline and glassy silicates. Solid State
427 Nuclear Magnetic Resonance, 5, 103-112.

428 Xue, X., and Kanzaki, M. (2009) Proton distributions and hydrogen bonding in crystalline and
429 glassy hydrous silicates and related inorganic materials: insights from high-resolution
430 solid-state nuclear magnetic resonance spectroscopy. Journal of American Ceramic
431 Society, 92, 2803-2830.

432 Zhao, Y., Zhao, X., and Ma, Z. (2006) Study on chronology for hot spring typed Cs-deposit of
433 Targejia, Tibet. Acta Petrologica Sinica, 22, 717-724.

434 Zhao Y. , Han, J., Guo, L., Qian, Z., Zhou, Y., Nie, F., and Li, Z. (2008) Characteristics and
435 geological significance of mineralogy and fabrics for the hot spring cesium deposit
436 occurring within the Targejia district, Tibet. Acta Petrologica Sinica, 24, 519-530.

437 Zheng, M. (1995) A new type of hydrothermal deposit: Cesium-bearing geyserite in Tibet.
438 Geological Press, Beijing.

439

Always consult and cite the final, published document. See http://www.minsocam.org or GeoscienceWorld

440

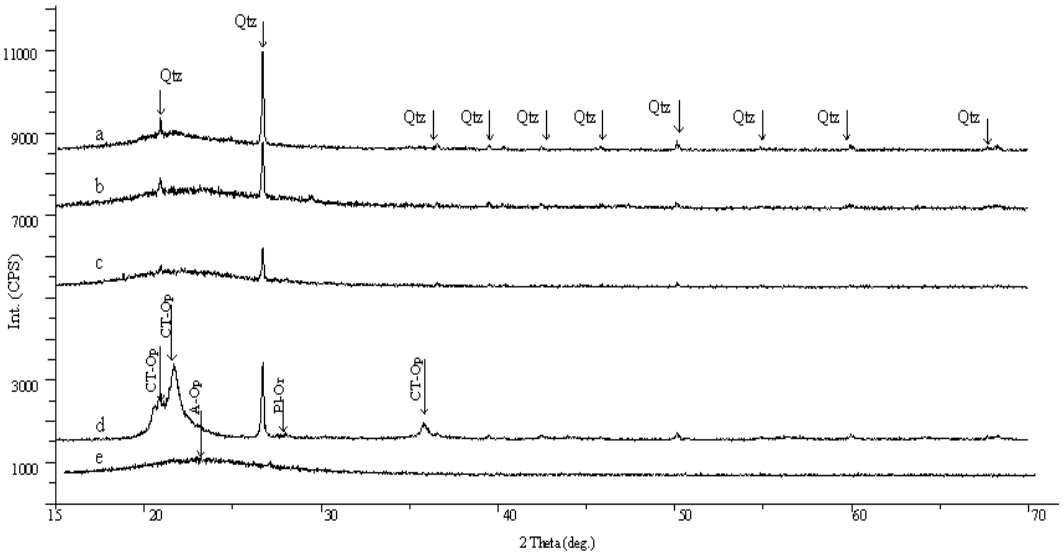

441

442 **Figure 1.** XRD patterns for the representative samples of the five mineralization stages (a:
443 stage 1 (Sample 8-3-10-3); b: stage 2 (Sample 8-3-8-1); c: stage 3 (Sample 8-3-4-1); d: stage
444 4 (Sample 8-3-1-1); e: stage 5 (Sample 8-3-2-18)). A-op: A-opal；CT-op: CT-opal；Qtz:
445 quartz；Pl-Or: Plagoioclase-Orthoclase

446

Always consult and cite the final, published document. See http://www.minsocam.org or GeoscienceWorld

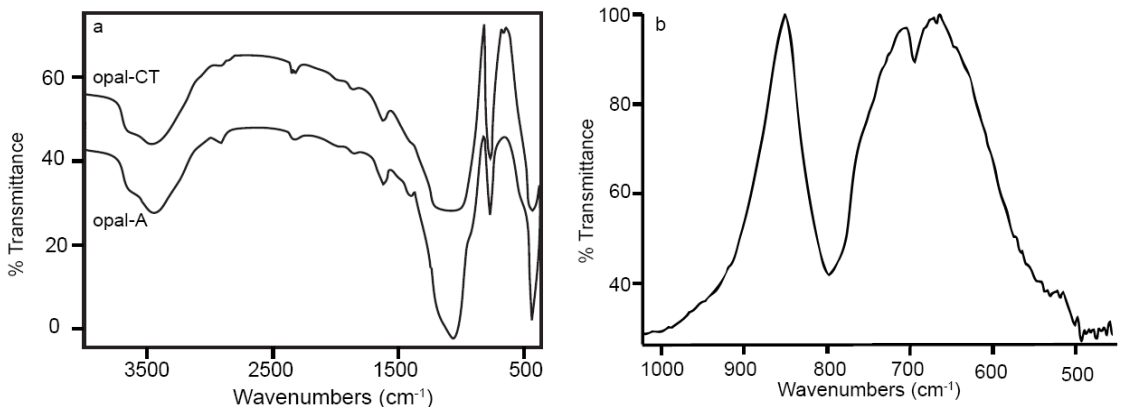

Figure 2. Infrared absorption spectra of (a) Cs-geyserite opal-CT (1st stage Sample 8-3-10-2) and opal-A (5th stage Sample 8-3-2-18) and (b) an enhanced region (1000 cm^{-1} to 400 cm^{-1}) of 2nd stage Sample 8-3-8-1.

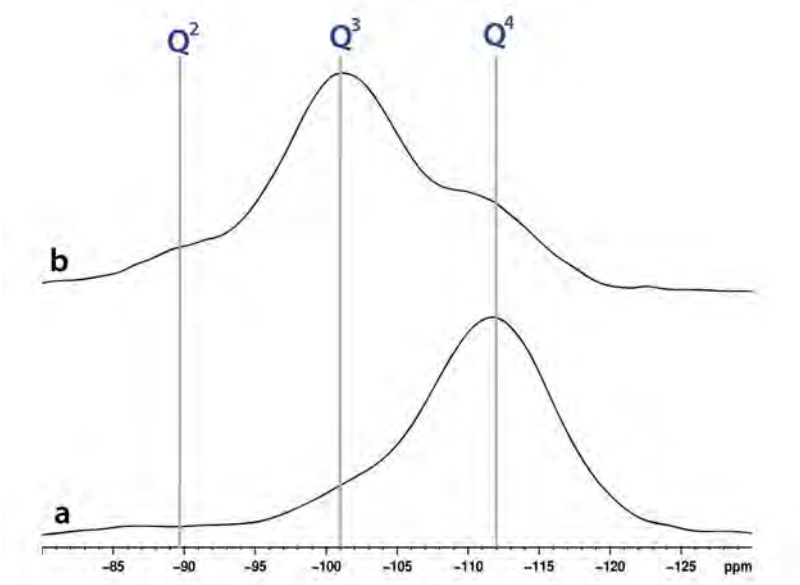

Figure 3. ^{29}Si MAS (a) and ^{1}H-^{29}Si CPMAS (b) NMR spectra for 3rd stage Sample 8-3-1-1 at 11.74 T (vertical lines for guiding eyes)

Always consult and cite the final, published document. See http://www.minsocam.org or GeoscienceWorld

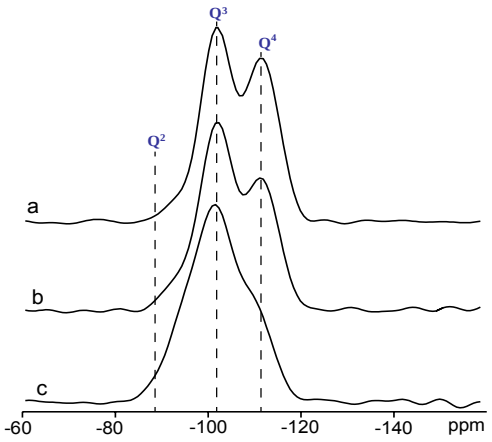

Figure 4. ^{1}H-^{29}Si CP MAS NMR spectra of Cs-geyserite sample 8-3-4-2 of 3rd stage at7.05 T (dash lines for guiding eyes). The three spectra represent different subsections from the sample: (a) top subsection, (b) middle subsection and (c) lower subsection.

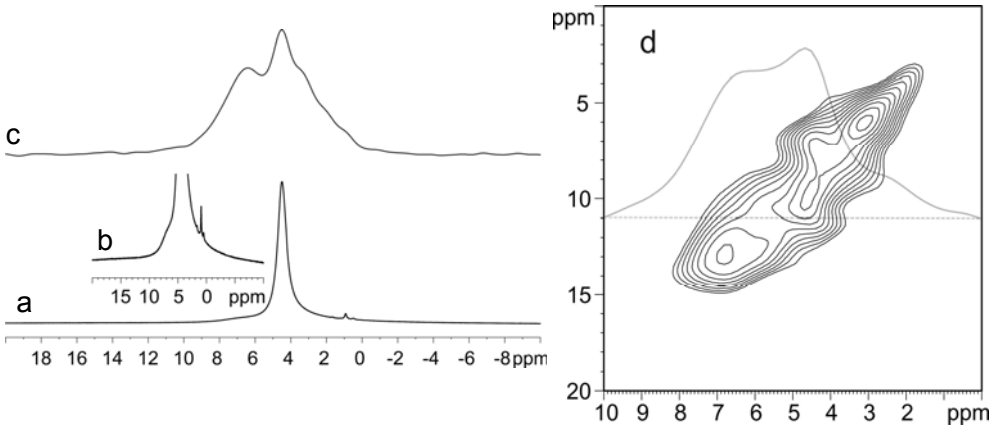

Figure 5. ^{1}H MAS NMR of Sample 8-3-2-30 of 5th stage using a Bloch decay (a), enhanced isotropic region (b) and a 1D slice of the DQ-filtered spectrum (c), and two-dimensional DQ-filtered spectrum acquired at 14.1 T (d), exhibiting a correlation between H_2O and OH^- groups (shown by the cross section).

Always consult and cite the final, published document. See http://www.minsocam.org or GeoscienceWorld

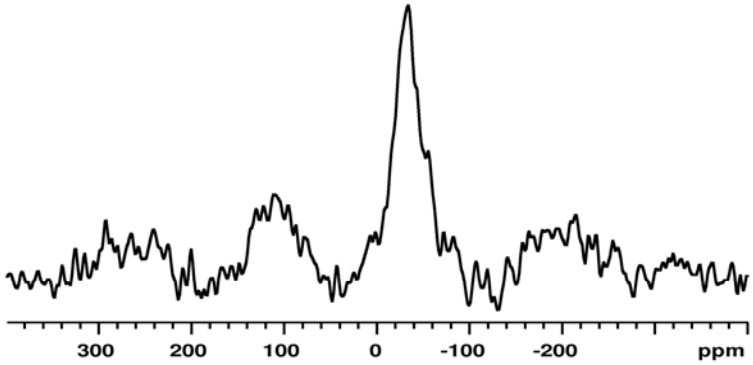

Figure 6. ^{133}Cs MAS NMR spectrum of Cs-Geyserite (Sample 8-3-1-1 of 3rd stage) at 14.1 T. Spinning side bands flanking the central transition (0 to -100 ppm) are present on either side.

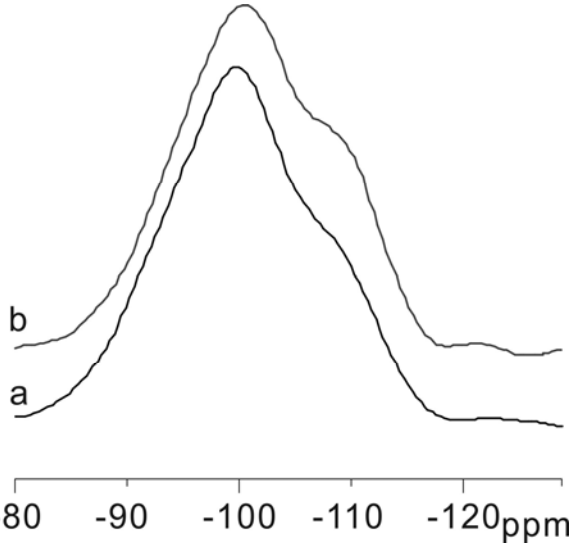

Figure 7. ^{1}H-^{29}Si CPMAS spectra for Sample 8-3-4-2 of 3rd stage at 7.05 T before (a) and after (b) stirring by the high-power ultrasonic vibration

Always consult and cite the final, published document. See http://www.minsocam.org or GeoscienceWorld

488

489

490 Table 1: The chemical compositions of the geyserite specimens (Zhao et al. 2006)

Sample number	8-3-10-2	8-3-5-2	8-3-4-2	8-3-1-3	8-3-2-30
Mineralization stage	1st stage	2nd stage	3rd stage	4th stage	5th stage
Na_2O	1.06	0.25	0.41	1.31	1.06
Al_2O_3		0.05			
SiO_2	94.10	96.53	97.51	92.18	89.71
K_2O	1.31	0.69	0.69	1.63	1.70
CaO	1.54	1.36	0.72	1.72	2.34
Cs_2O	0.99	0.57	0.67	1.75	2.60
$\sum(Na_2O+Al_2O_3+ K_2O +CaO)$	3.91	2.35	1.82	4.66	5.1

491

492

Always consult and cite the final, published document. See http://www.minsocam.org or GeoscienceWorld